

Nuclear medium cooling scenario in the light of new Cas A cooling data and the $2 M_{\odot}$ pulsar mass measurements

D. Blaschke,^{1,2} H. Grigorian,^{3,4} and D. N. Voskresensky⁵

¹*Institute for Theoretical Physics, University of Wrocław, 50-204 Wrocław, Poland*

²*Bogoliubov Laboratory for Theoretical Physics, Joint Institute for Nuclear Research, 141980 Dubna, Russia*

³*Department of Theoretical Physics, Yerevan State University, 375025 Yerevan, Armenia*

⁴*Laboratory for Information Technologies, Joint Institute for Nuclear Research, 141980 Dubna, Russia*

⁵*National Research Nuclear University (MEPhI), 115409 Moscow, Russia*

(Dated: November 3, 2018)

Recently, Elshamouty et al. performed a reanalysis of the surface temperature of the neutron star in the supernova remnant Cassiopeia A on the basis of Chandra data measured during last decade, and added a new data point. We show that all reliably known temperature data of neutron stars including those belonging to Cassiopeia A can be comfortably explained in our "nuclear medium cooling" scenario of neutron stars. The cooling rates account for medium-modified one-pion exchange in dense matter, polarization effects in the pair-breaking-formation processes operating on superfluid neutrons and protons paired in the $1S_0$ state, and other relevant processes. The emissivity of the pair-breaking-formation process in the $3P_2$ state is a tiny quantity within our scenario. Crucial for a successful description of the Cassiopeia A cooling proves to be the thermal conductivity from both, the electrons and nucleons, being reduced by medium effects. Moreover, we exploit an EoS which stiffens at high densities due to an excluded volume effect and is capable of describing a maximum mass of $2.1 M_{\odot}$, thus including the recent measurements of PSR J1614-2230 and PSR J0348+0432.

PACS numbers: 97.60.Jd, 95.30.Cq., 26.60.-c

I. INTRODUCTION

The isolated neutron star in Cassiopeia A (Cas A) was discovered in 1999 by the *Chandra* satellite [1]. Its association with the historical supernova SN 1680 [2] gives Cas A an age of 333 years, in agreement with the nebula's kinematic age [3]. The thermal soft X-ray spectrum of Cas A can be fitted with a non-magnetized carbon atmosphere model, a surface temperature of 2×10^6 K, and an emitting radius of 8 to 17 km [4]. Analyzing the data from 2000 to 2009, Heinke & Ho [5] reported a rapid decrease of Cas A's surface temperature over a 10-year period, from 2.12×10^6 to 2.04×10^6 K. Such a rapid drop in temperature conflicts with standard cooling scenarios based on the efficient modified Urca (MU) process [6, 7]. Interpretations of Cas A's temperature data based on hadronic matter cooling scenarios were provided by Page *et al.* [8], Yakovlev *et al.* [9, 10], Blaschke *et al.* [11]. The new analysis of the *Chandra* data performed by Elshamouty *et al.* [12] including a new measured data point allowed to precisely extract the decade temperature decline. The drop in the temperature lies in the range 2...5.5%, and the most recent results from ACIS-S detector yield a 3...4% decline.

The interpretation of Cas A data by Page *et al.* [8] is based on the "minimal cooling" paradigm [13], where a minimal number of cooling processes is taken into account. These are photon emission, the MU process, nucleon-nucleon (NN) bremsstrahlung (NB) and the neutron (n) and proton (p) pair breaking-formation processes (nPBF and pPBF). To calculate the NN interaction entering the emissivities of the MU and NB processes the minimal cooling scenario employs the free one-pion

exchange (FOPE) model [14]. As shown in [8], the Cas A data can be reproduced by assuming a large value for the proton pairing gap throughout the entire stellar core. The latter assumption facilitates additional suppression of the emissivity of the MU and the pPBF processes. Under this assumption the nPBF reaction in the core, where neutrons are paired in $3P_2$ state, proves to be the most efficient one. The authors describe Cas A data by fixing the critical temperature for the neutron $3P_2$ pairing gap at around 0.5×10^9 K. The result is mildly sensitive to the neutron star mass. Surface temperature-age data of other neutron stars, which do not lie on the cooling curve of Cas A, are explained within the minimal cooling scenario mainly by assuming variations in the light element mass of the envelopes of these stars. However both, younger neutron stars like the one in CTA1, and very old hotter stars require more than minimal cooling [15].

The works of Yakovlev *et al.* [9, 10] include all emission processes which are part of the minimal cooling paradigm including the FOPE model for MU reaction rate. They assume that the proton gap is so large that charged current processes are strongly suppressed in the entire stellar core. The value and the density dependence of the $3P_2$ neutron gap are fitted to the Cas A data, leading to a critical temperature of $0.7 \dots 0.9 \times 10^9$ K for the neutron pairing gap and a neutron star mass $M = 1.65 M_{\odot}$. Both groups therefore came to the striking conclusion that the temperature data of Cas A allow one to extract the value of the $3P_2$ neutron pairing gap. Continuing this approach Elshamouty *et al.* [12] arrive at the same conclusion.

The work of Blaschke *et al.* [11] presents the "nuclear medium cooling scenario" as a model for the suc-

cessful description of all the known temperature data including those of Cas A. This scenario includes efficient medium modified Urca (MMU) and medium nucleon bremsstrahlung (MnB, MpB) processes, as motivated by a softening of the virtual pion mode in dense matter [16, 17], a very low (almost zero) value of the $3P_2$ neutron gap, as motivated by the result of Schwenk and Friman [18], and a small thermal conductivity of neutron star matter caused by in-medium effects, as motivated by calculations of the lepton thermal conductivity of Shternin and Yakovlev [19] and evaluations of the effect of pion softening on the nucleon thermal conductivity. More specifically, in [11] we just used values of the thermal conductivity calculated by Baiko *et al.* [20] suppressed by a parameter ζ_κ . The best fit of Cas A data was performed for $\zeta_\kappa = 0.265$. A strong suppression of the thermal conductivity is justified by results of Shternin and Yakovlev [19], who included the in-medium effect of Landau damping of electromagnetic interactions owing to the exchange of transverse plasmons in the partial electron (and muon) contribution to the thermal conductivity. Earlier, this effect has been studied by Heiselberg and Pethick for a degenerate quark plasma [21] and by Jaikumar *et al.* [22] for neutrino bremsstrahlung radiation via electron-electron collisions in neutron star crusts and cores. Now, we incorporate the in-medium modifications of the electron-electron interaction into our scenario, precisely as it has been done in [19]. Moreover, the partial NN thermal conductivity should be suppressed within our scenario owing to the increase of the squared NN interaction matrix element with density caused by the medium modification of the FOPE. Thereby, we additionally suppress the NN thermal conductivity term calculated in [20] by taking into account the softening of the one-pion exchange for this quantity as well as for all processes considered in our scenario.

As the nuclear matter equation of state (EoS), in [11] we used the Heiselberg-Hjorth-Jensen (HHJ) EoS [23] (with a fitting parameter $\delta = 0.2$) that fits the microscopic Akmal-Pandharipande-Ravenhall (APR) $A18 + \delta v + UIX^*$ EoS [24] for symmetric nuclear matter up to $4n_0$, where $n_0 = 0.16 \text{ fm}^{-3}$ is the nuclear saturation density. This yields an acceptable (although not perfect) fit of the APR EoS of neutron star matter for those densities. The maximum neutron star mass calculated with the HHJ($\delta = 0.2$) EoS, $M_{\text{max}} = 1.94 M_\odot$, proves to be smaller than the one calculated with the original APR EoS, $M_{\text{max}} \simeq 2.2 M_\odot$. However, the latter EoS becomes acausal for $n > 0.86 \text{ fm}^{-3}$, whereas all HHJ($\delta \geq 0.13$) EoS respect causality at all densities. Recent measurements of two massive neutron stars, with $M_{1614} = 1.97 \pm 0.04 M_\odot$ for PSR J1614-2230 [25] and $M_{0348} = 2.01 \pm 0.04 M_\odot$ for PSR J0348-0432 [26], motivate us to use a stiffer EoS than that of HHJ($\delta = 0.2$) at large densities. In the present work we modify the EoS in order to fulfill the new observational constraints on masses of neutron stars. To that end we incorporate excluded volume corrections in the HHJ($\delta = 0.2$) EoS such

that it would remain unchanged for $n \lesssim 4n_0$ but would become stiffer for higher densities.

Thus our aim in the given work is to demonstrate the efficiency of our nuclear medium cooling scenario in explaining the cooling data introducing the lepton contribution to the thermal conductivity following [19] and extending the HHJ($\delta = 0.2$) EoS to describe the new data on massive stars.

II. NUCLEAR MEDIUM COOLING SCENARIO

The nuclear medium cooling scenario worked out in Refs. [17, 27–30] has been successfully applied to the description of the body of known surface temperature–age data of neutron stars [11, 31–34]. It exploits a strong dependence of the main cooling mechanisms on the density and thus on the neutron star mass.

A. Free versus medium-modified one-pion-exchange in dense matter

We exploit the Fermi liquid approach, where the short-range interaction is treated with the help of phenomenological Landau-Migdal parameters, whereas long-range collective modes are explicitly presented. The most important effect comes from the mode with the pion quantum numbers treated explicitly, as it is a soft mode ($m_\pi \ll m_N$, with m_π (m_N) being the pion (nucleon) mass). The key effect is the softening of the pion mode with increasing density [16, 17]. Only with the inclusion of this softening effect the phase transition to a pion condensation state in dense nucleon matter may appear. Thus it is quite inconsistent to use FOPE model for description of NN -interaction and simultaneously include processes going on pion condensation.

The insufficiency of the FOPE model for the description of the NN -interaction is a known issue. Actually, using the FOPE for the NN interaction amplitude, and simultaneously considering pion propagation as free, violates unitarity. Indeed, calculating the MU emissivity perturbatively one may use both the Born NN interaction amplitude given by the FOPE and the optical theorem, considering the imaginary part of the pion self-energy [27–29]. In the latter case, at low densities one needs to expand the exact pion Green's function $D_\pi(\omega, k) = [\omega^2 - m_\pi^2 - k^2 - \Pi(\omega, k, n)]^{-1}$ to second order using for the polarization function $\Pi(\omega, k, n)$ the perturbative one-loop diagram, $\Pi_0(\omega, k, n)$. For $k = k_0$, which is the pion momentum at the minimum of the effective pion gap defined as $\omega^{*2} = -D_\pi^{-1}(\omega = 0, k = k_0)$, the polarization function $\Pi_0(\omega, k = k_0 \simeq p_{F,n}, n)$ yields a strong P -wave attraction. Here $p_{F,n}$ is the neutron Fermi momentum. This attraction proves to be so strong that it would trigger a pion condensation instability already at low baryon densities of $n \sim 0.3n_0$, which is in disagreement with experimental data on atomic nuclei at

the nuclear saturation density n_0 . Note that the perturbative calculation contains no one free parameter. The paradox is resolved by observing that together with pion softening (i.e., a decrease of the effective pion gap $\omega^*(n)$ with increasing density for $n > n_{cr}^{(1)}$, $\omega^{*2}(n_{cr}^{(1)}) = m_\pi^2$) one needs to include a short-range repulsion arising from the dressed πNN vertices, $\Gamma(n) \simeq [1 + C(n/n_0)^{1/3}]^{-1}$ with $C \simeq 1.6$. This evaluation exploits an estimated value of the Fermi-liquid spin-spin Landau-Migdal parameter g and the Lindhard function taken in the limit of low transferred energy $\omega \ll p_{F,n}$. A consistent description of the NN interaction in matter should thus use a medium modified one-pion exchange (MOPE) interaction characterized by the fully dressed pion Green function, dressed vertices $\Gamma(n)$, and a residual NN interaction. We stress that dressing the pion mode is similar to the ordinary dressing of the photon mode in a plasma. Computing similar diagrams results in a dispersion of the dielectric constant $\varepsilon(\omega, q) \neq 1$, i.e. it might essentially deviate from unity. Moreover, only by including dressed vertices one is able to describe zero sound modes in Fermi liquids. Microscopic calculations of the residual interaction are very cumbersome. However, according to evaluations in [17, 27], the main contribution for $n > n_0$ is given by MOPE, whereas the relative contribution of the residual interaction diminishes with increasing density owing to polarization effects. Thus, in our simplified treatment the main dependence on the short-range interaction enters MOPE via the phenomenological vertex suppression factor $\Gamma(n)$.

The density dependence of the effective pion gap ω^* that we use for $n > n_{cr}^{(1)}$, taken to be $0.8 n_0$, is demonstrated in Fig. 1 (Fig. 1 of [32]). The curve 1a in Fig. 1 shows behavior of the pion gap for $n < n_{cr}^\pi$, where n_{cr}^π , taken to be $3n_0$, is the critical density for the pion condensation. For simplicity we do not distinguish between different possibilities of π^0 , π^\pm condensations, see [17] for a more general description. Note that variational calculations of Akmal *et al.* [24] produce still smaller critical densities for the charged and neutral pion condensations. However, in order to be conservative we assume a larger value of n_{cr}^π . Following the model used here and in [32, 33] within the HHJ($\delta = 0.2$) EoS, the pion condensation arises for neutron star masses $M \geq 1.32 M_\odot$ (corresponding to the choice $n \geq n_{cr}^\pi = 3n_0$). The curve 1b demonstrates the possibility of a saturation of pion softening and absence of the pion condensation for $n > n_{cr}^\pi$ (this possibility could be realized, e.g., if the Landau-Migdal parameters increased with the density). Thus the curves 1a+1b determine behavior of the Green function for the pion excitations in absence of condensation. Curves 2, 3 demonstrate possibility of the pion condensation for $n > n_{cr}^\pi$. The continuation of the branch 1a for $n > n_{cr}^\pi$, called branch 2, shows the reconstruction of the pion dispersion relation in the presence of the condensate state. In the presence of the pion condensate (for $n > n_{cr}^\pi$) the value ω^* from curve 2 enters the emissivities of all processes with pion excitations in initial, interme-

mediate and final reaction states. In agreement with the general trend known in condensed matter physics, fluctuations dominate in the vicinity of the critical point of the phase transition (where ω^* has its smallest values) and die out far away from it. In strongly interacting systems, like ^4He , fluctuations prove to be important at all temperatures. The jump from branch 1a to branch 3 at $n = n_{cr}^\pi$ is due to the first order phase transition to the π condensation, see [17]. The $|\omega^*|$ value on branch 3 is proportional to the amplitude of the pion condensate mean field. To avoid misunderstanding we stress that, although to construct the curves $\omega^*(n)$ we used available experimental information and well established general principles [17], the quantitative density dependence of $\omega^*(n)$ remains essentially model dependent due to a lacking knowledge of the NN interaction in neutron star matter at large densities. Thus we hope that our successful description of the neutron star cooling may be helpful to correctly choose the parameterization of the interaction.

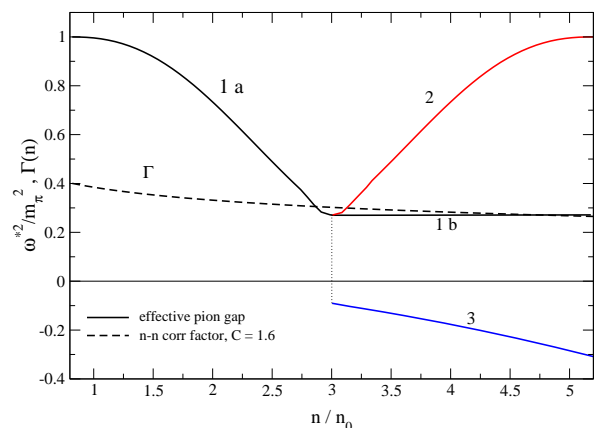


FIG. 1: (Color online) Square of the effective pion gap ω^* with pion condensation (branches 1a+2 and 3) and without (1a+ 1b). $\Gamma(n)$ is the nucleon - nucleon correlation factor.

The direct Urca (DU) process, $n \rightarrow pe\bar{\nu}$, is too efficient for a description of the full set of neutron star cooling data. Moreover, the DU process occurs only for high proton fractions, $x_p = n_p/n > 0.11 \dots 0.14$. In the calculation of the neutrino emissivity of two-nucleon processes, e.g., $nn \rightarrow npe\bar{\nu}$, not only radiation from the nucleon legs but also from intermediate reaction states is allowed. For $n \gtrsim n_0$, the latter processes prove to be more efficient than the ordinary MU process from the legs. With such an interaction the ratio of the emissivity of the medium modified Urca (MMU) to the MU process, see [11, 32, 33],

$$\frac{\epsilon_\nu[\text{MMU}]}{\epsilon_\nu[\text{MU}]} \sim 3 \left(\frac{n}{n_0} \right)^{10/3} \frac{[\Gamma(n)/\Gamma(n_0)]^6}{[\omega^*(n)/m_\pi]^8}, \quad (1)$$

strongly increases with density for $n \gtrsim n_0$. For $n < n_{cr}^{(1)}$ we use $\epsilon_\nu[\text{MU}]$ as in the minimal cooling scenario. Although an increase of the ratio of the emissivities of the medium modified nucleon (neutron) bremsstrahlung process (MnB) to the unmodified bremsstrahlung (nB) is less pronounced, the MnB process, being not affected by the proton superconductivity, may yield a relatively large contribution in the region of a strong proton pairing. Note that being computed with values ω^* and Γ , which we use, the ratio of the MOPE NN cross section to that of the FOPE [29] proves to be $\sigma[\text{MOPE}]/\sigma[\text{FOPE}] \sim 1/3 \dots 1/2$ for $n = n_0$ but it increases with increasing density. The subsequent increase of the cross section with density is due to the dominance of the softening of the pion mode owing to πNN and $\pi N \Delta^*(1236)$ P -wave attraction compared to the suppression of vertices owing to repulsive NN correlations [17, 29]. Thus the known suppression of the in-medium NN cross section at $n \lesssim n_0$ compared to that given by the FOPE [35, 36] does not conflict with a strong enhancement of the MMU emissivity with increasing density. Estimated strong density dependence of the in-medium neutrino-processes motivated authors of [27] to suggest that difference in surface temperatures of neutron stars is explained by different masses of the objects (that time only upper limits on surface temperatures were put). At the end, we should stress that in order to explain the cooling of both slowly and rapidly cooling stars one requires neutrino emissivities that differ by a factor $> 10^3$. Therefore, an uncertainty of the order of one in the emissivity of the processes does not affect the general cooling picture.

B. Gaps and pair-breaking-formation

In spite of many calculations performed so far, the values of nucleon gaps in dense neutron star matter remain poorly known. This is a consequence of the exponential dependence of the gaps on the potential of the in-medium NN interaction. The latter potential is not sufficiently well known. Gaps that we have adopted in the framework of the nuclear medium cooling scenario are presented in Fig. 2 (cf. Fig. 5 of [32]).

The $\Delta_{nn}(^1S_0)$ neutron gap is taken from [37]. As follows from the analysis of [33] the cooling proved to be not much sensitive to the value and density dependence of the 1S_0 neutron gap mainly since the pairing is restricted to the region of rather low densities. Two different models [32, 33], labeled I and II, are used for the proton gap $\Delta_{pp}(^1S_0)$, which is spread up to larger densities. Model I is a fit from [38] and model II is a calculation from [39]. Refs. [11, 33] demonstrate a strong sensitivity of the cooling to the values and the density dependence of the proton gap. For $n \lesssim 0.8 n_0$ neutrons are paired in the 1S_0 state and for larger n , in the $3P_2$ state. For densities up to $3 \dots 4 n_0$ protons are paired in the 1S_0 state.

An important in-medium effect which we incorporated in our nuclear medium cooling scenario is the very strong

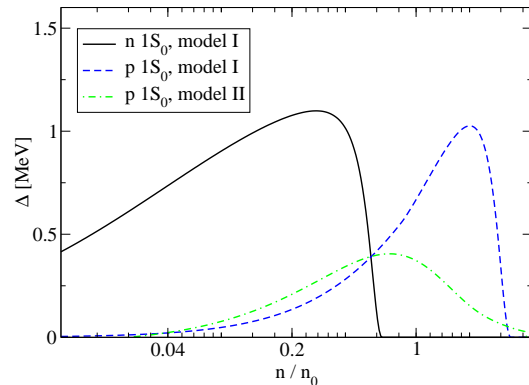


FIG. 2: (Color online) Neutron and proton 1S_0 pairing gaps. The 1S_0 neutron gap is shown as the bold solid line. The 1S_0 proton gap is given for model I (dashed line) and for model II (dash-dotted line). The tiny value of the $3P_2$ gap is not shown.

suppression of the neutron $3P_2$ pairing gap $\Delta_{nn}(3P_2)$, as motivated by detailed calculations of Ref. [18]. According to this analysis, with due account of polarization effects the gap turns out to be $\Delta_{nn}(3P_2) \lesssim \text{few keV}$, i.e., it is dramatically suppressed compared to BCS based calculations [39]. Ref. [33] exploiting various simulations concluded that within our cooling scenario the $3P_2$ gap should be suppressed compared to values $(0.2 \dots 0.5) \cdot 10^9 \text{K}$ used by [38, 39]. Thus we adopt a tiny $\Delta_{nn}(3P_2)$ gap following [18]. Actually, the value of the gap that yields the best fit of Cas A data within our scenario is so tiny [33] that it does not affect the cooling evolution. Therefore, we do not show $\Delta_{nn}(3P_2)$ in Fig. 2.

Furthermore, as it is commonly accepted, the neutron and proton superfluidities cause an exponential suppression of neutrino emissivities of the nucleon processes and of the nucleon specific heat and open up the new class of nPBF and pPBF processes. The nPBF neutrino process was introduced in [28, 40], the pPBF one, in [28]. Their important effect on the cooling was first incorporated in a cooling code in Ref. [31]. Afterwards, these processes were used in all relevant cooling codes. The important role of polarization effects in pPBF and nPBF processes was first noted in [28]. Detailed analyses of the vector current conservation in PBF reactions [41, 42] have shown that by taking the in-medium dressing of vertices into account, as it is required by the Ward-Takahashi identities, the emissivity of processes on the vector current proves to be dramatically suppressed $\propto v_F^4$, where v_F is the Fermi velocity. Consequently, the main contribution to the PBF emissivity comes from processes on the axial current, suppressed only as $\propto v_F^2$, [42]. For the ratio of the proton to the neutron PBF emissivities we may estimate [42]

$$R[p/n] \sim x_p^{4/3} (\Delta_p/\Delta_n)^{13/2} e^{2(\Delta_n - \Delta_p)/T} \quad (2)$$

in the low temperature limit where $T \ll T_{cp}, T_{cn}$. Here Δ_n and Δ_p are the neutron and proton $1S_0$ gaps while T_{cp} and T_{cn} are corresponding critical temperatures. The emissivities of the PBF processes are computed following expressions given in Ref. [42]. The emissivities of the two-nucleon processes are suppressed in the presence of the pairing by the R -factors presented, e.g., in Ref. [6].

Concluding this subsection we stress that there are many calculations of the $1S_0$ neutron and proton gaps and there are some evaluations of $3P_2$ neutron gaps, for references see, e.g., [43–49]. We used the same two choices of the gaps as in our previous works [32, 33] just to demonstrate the efficiency of the predictions of our old model. If we used results of other calculations of $1S_0$ neutron and proton gaps we could explain the cooling data tuning some not well known parameters, such as the quantities Γ and $\tilde{\omega}$ entering the MMU emissivity. The results are sensitive to the value and the density dependence of the $3P_2$ neutron gap mainly because it spreads to large densities. Ref. [50] discussed the interesting possibility of a large $3P_2$ neutron gap (exceeding ~ 1 MeV). With such a gap the region with $n > n_c(3P_2)$ would be excluded from the cooling due to a strong (exponential) suppression of the emissivities of the processes for $T \lesssim 10^9$ K of our interest. Usually, one considers $3P_2$ pairing to occur for $n \gtrsim n_0$. Such densities are already reached in the center of a neutron star with mass $M \sim 0.3 M_\odot$, see Fig. 4 below, whereas we have no observations of neutron star masses lower than $\sim 1.1 M_\odot$. Thereby, and as we have shown in [33], within our scenario we could not succeed to get an appropriate fit of the data, if $3P_2$ neutron gaps were large in a broad density interval.

C. The thermal conductivity

We also want to stress that the thermal conductivity, being essential for the cooling of young objects such as Cas A [11], strongly depends on in-medium effects like the Landau damping effect in the electron term and effect of an increase of the NN interaction amplitude with the density owing to MOPE. These effects are now consistently included in our calculation scheme.

The thermal conductivity κ is given by the sum of partial contributions, $\kappa = \kappa_b + \kappa_l$, where κ_b is the heat conductivity of baryons (mainly neutrons) and κ_l , of leptons (mainly electrons). The ep crossing term entering κ_l proves to be small [19]. In [32] and [38] the electron and nucleon thermal conductivities were computed according to the analysis of [20]. More recent studies [19] showed that the lepton thermal conductivity is reduced by an order of magnitude. Moreover, as we argued in [32], pion softening effects may additionally suppress the baryon contribution κ_b to the thermal conductivity.

The impact of a low thermal conductivity on the thermal evolution of neutron stars accomplished by introducing a factor $\zeta_\kappa = 0.3$ was first demonstrated in Fig. 17

of [32]. The net effect is a delay of the temperature decline for young ($\lesssim 300$ yr) neutron stars. This idea of a possible strong suppression of the thermal conductivity allowed for the explanation of the rapid cooling of Cas A in [11]. In the given work we use the lepton contribution to the thermal conductivity from [19], cf. Eqs. (40) and (93) of that work. One may parameterize the result of [19] as

$$\kappa_e = 8.5 \cdot 10^{21} \left(\frac{p_{F,e}}{\text{fm}^{-1}} \right)^2 f_e \text{ ergs s}^{-1} \text{ cm}^{-1} \text{ K}^{-1}, \quad (3)$$

$$f_e \simeq \frac{2.7}{e^{1.3T/T_{cp}} - 1},$$

for $T < T_{cp}$ and $f_e = 1$ for $T > T_{cp}$. For simplicity a contribution of muons is neglected.

In order to include the effect of the softening of the pion exchange on κ_b we recalculate the S_{12} factors of [20] first with FOPE and then with MOPE and from their ratio we construct an extrapolation for κ_b , which takes into account of the pion softening effect for $n > n_{cr}^{(1)}$. Finally we replace

$$\kappa_b = \kappa_b^{\text{SY}} (\omega^*(n)/m_\pi)^3 (\Gamma(n_0)/\Gamma(n))^4 n_0/n, \quad (4)$$

where κ_b^{SY} is the result of [19]. Note that the main contribution to the thermal conductivity comes from electrons and we could use κ_b^{SY} for the baryons to get appropriate fit of Cas A. We introduce a suppression of κ_b^{SY} since it is in a line with our general argumentation about softening of the NN interaction owing to the in-medium pion exchange.

D. Blanketing envelope

In our model the processes occurring in dense neutron star matter are typically much more efficient than those considered within minimal cooling modeling. Thus within our scenario the cooling is mainly determined by the reactions in the neutron star interior and much less sensitive to the modeling of the crust. The presence of a pasta phase [51] at $0.3 \lesssim n/n_0 \lesssim 0.8$ could partially influence the cooling [52] and the heat conduction due to the possibility of efficient DU-like neutrino processes. These might be occurring with the participation of non-uniform structures [53], in spite of the fact that the free proton fraction disappears in pasta. However, processes in this phase are badly studied. Thereby this phase is continuing to be ignored in the cooling simulations. Thus due to ambiguities of its description we ignore the possibility of the presence of a pasta layer in our calculations.

The cooling curves essentially depend on the relation between the internal and surface temperature at small densities $\sim 10^{-3}n_0$ in the blanketing envelope. This relation is not unique and depends on the mass ΔM and the structure of the blanketing envelope. In our works we use the same band for $T_s - T_{in}$, as it was presented in [54].

In [32, 33] we demonstrated the dependence of the cooling curves on different choices of fits $T_s = f(T_{in})$ within the band and then focused on a model called “our fit”, which assumes that for cold more massive neutron stars the parameter $\eta = \Delta M/M$ is smaller than for hotter less massive stars. Thus we use a fitting curve $T_s = f(T_{in})$ matching two regimes between $\eta = 4 \cdot 10^{-16}$ and $\eta = 4 \cdot 10^{-8}$. This “our fit” curve is rather close to a known simplified Tsuruta law. Note that for the mass $\sim 1.5 M_\odot$ “our fit” model yields an η value similar to the one used to explain Cas A cooling in [8].

E. Equation of state and massive stars

As we have mentioned, we adopted the HHJ($\delta = 0.2$) EoS for the description of the nucleon contribution. The energy density of nucleons is parameterized as follows

$$E_N = un_0 \left[m_N + e_B u \frac{2 + \delta - u}{1 + \delta u} + a_{\text{sym}} u^{0.6} (1 - 2x_p)^2 \right], \quad (5)$$

where $u = n/n_0$, $e_B \simeq -15.8$ MeV is the nuclear binding energy per nucleon, $a_{\text{sym}} \simeq 32$ MeV is the symmetry energy coefficient and we chose $\delta = 0.2$. With these values of parameters one gets the best fit of APR (A18+ δv +UIX*) EoS for symmetric nuclear matter up to $n \sim 4 n_0$. The nucleon effective masses are taken as for the APR EoS. As we have mentioned, with such E_N one reaches the value of the maximum mass of the neutron star $M_{\text{max}} = 1.94 M_\odot$, less than recently measured values of masses of pulsars PSR J1614-2230 and PSR J0348-0432. The value of the maximum mass can be easily increased within the HHJ approach provided one diminishes the parameter δ . However, then one spoils the best fit to the microscopic APR (A18+ δv +UIX*) EoS. To preserve the best fit to the APR (A18+ δv +UIX*) EoS for $n \lesssim 4 n_0$ we should perform modifications of EoS only for $n > 4 n_0$. To do this we exploit the idea of an excluded volume, related to the quark substructure of the nucleons and the Pauli exclusion principle on the quark level. Thus, making use of the replacement

$$u \rightarrow \frac{u}{1 - \alpha u e^{-(\beta/u)^\sigma}} \quad (6)$$

in the expression for the energy per particle (in squared bracket of Eq. (5)) we incorporate the excluded volume effect. We take $\alpha \equiv n_0 v_0 = 0.02$, $\beta = 6$ and $\sigma = 4$, where v_0 has the meaning of an excluded volume. Thus we derive a new phenomenological HDD EoS. Note that our parameter choice corresponds to the radius of the quark core of the nucleon $r_q \simeq 0.2 \dots 0.3$ fm.

In principle pion condensation, if it occurs for $n > n_{cr}^\pi$, softens the EoS. However, the value of this softening is essentially model dependent. Therefore, to diminish the dependence of the EoS on unknown parameters we disregard a possible influence of pion condensation on the EoS. Also, we suppress possible effect of hyperonization on EoS.

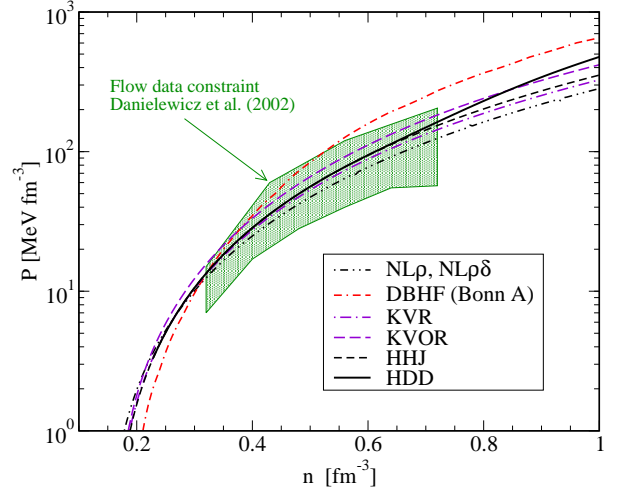


FIG. 3: (Color online) Pressure as function of density consistent with a constraint extracted from experimental flow data in isospin symmetric nuclear matter [55] (dark shaded region). The HDD EoS (bold solid line) is introduced in this work, while other EoSs shown for comparison are used according to Ref. [56] and the notation introduced there.

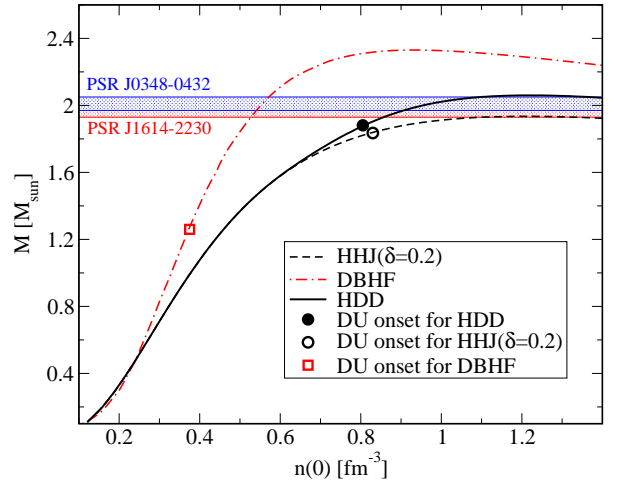


FIG. 4: (Color online) Neutron star mass vs. central density for HHJ($\delta = 0.2$) (dashed line), DBHF (dash-dotted line) and HDD (bold solid line) EoSs. Symbols on the lines indicate the thresholds of the DU reaction.

In Fig. 3 we compare different EoS models for isospin-symmetric nuclear matter with a constraint region extracted from an analysis of experimental flow data [55]. It is seen that both, the HHJ($\delta = 0.2$) and the HDD EoSs satisfy the experimental constraint (shaded region). The HDD EoS stiffens only for $n > 4 n_0$. Causality is not violated up to the limiting central density for stable neutron stars.

In Fig. 4 we show neutron star masses vs. central density $n(0)$ for HHJ($\delta = 0.2$), DBHF and HDD EoSs. With

our parameter choice the HDD EoS produces a maximum mass $M_{\text{max}} = 2.06 M_{\odot}$. The DU threshold is changed only slightly compared to that for the HHJ($\delta = 0.2$) EoS while DBHF has a very early DU onset.

Note that our HDD EoS might be rather convenient for the description of possible phase transitions, like the hadron – quark phase transition, in massive neutron stars. The latter transition may occur as a first or second order phase transition, as a crossover, or as the melting of hadron matter, when the quark cores of hadrons become essentially overlapping. At $n > 4n_0$ the hadron pressure additionally increases compared to that for HHJ EoS, which favors the transition to quark matter at a smaller pressure for fixed baryon chemical potential.

III. NEUTRON STAR IN CAS A

The ingredients of the nuclear medium cooling scenario discussed above lead to neutron star cooling curves in Fig. 17 of Ref. [32], where model I for the proton gap has been adopted and the role of the thermal conductivity on the hot early stages of hadronic neutron star cooling was elucidated (see curves for $\kappa = 0.3$ in [32]). In Fig. 1 of [11] we redrew those cooling curves permitting readjustment of the thermal conductivity parameter. This allowed us to describe all cooling data including those for Cas A, known at that time.

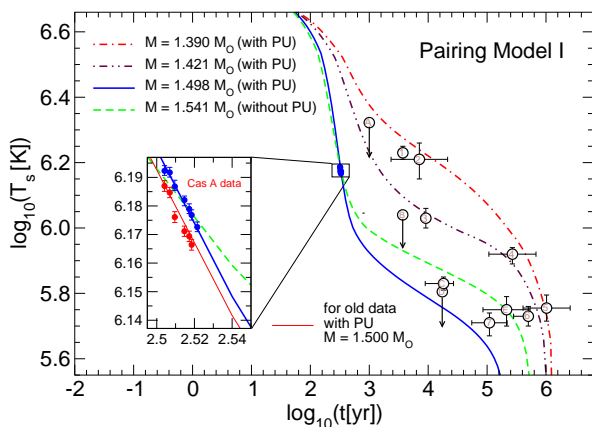


FIG. 5: (Color online) Cooling of neutron stars within nuclear medium cooling scenario, with PU and without PU for model I for pairing, cf. also Fig. 17 of [32] and Fig. 1 of [11]. Data from Refs. [9, 13]. New data for Cas A (above the old ones) from [12].

In Fig. 5 we show results of our new calculation for the model I for pairing, with pion condensation (with PU), see curves 1a+2 and 3 in Fig. 1, and without pion condensation (without PU), see curves 1a+1b in Fig. 1. As we mentioned, we use *all* the same parameters, as

in our previous calculation [11] but instead of an *ad hoc* suppression of κ we now exploit calculated values of κ , cf. Eqs. (3), (4) above. The change of κ affects the cooling of young objects ($t \lesssim 300$ yr) only.

With PU we perfectly explain the new Cas A data for $M = 1.498 M_{\odot}$ and the old Cas A data for $M = 1.500 M_{\odot}$ (in [11] we had $M = 1.463 M_{\odot}$ and $\zeta_{\kappa} = 0.265$). As is seen from Fig. 5, with the neutron star mass $M = 1.390 M_{\odot}$ the upper data points are covered. The lower data points are covered for the mass of Cas A. Thus the whole set of available cooling data is covered with masses in the range $1.390 < M/M_{\odot} < 1.5$.

Assuming the absence of pion condensation in the core of a neutron star (model “without PU”), the new Cas A cooling data are described for $M = 1.541 M_{\odot}$ whereas for $M = 1.500 M_{\odot}$ the old Cas A data are reproduced (in [11] we had for this case $M = 1.532 M_{\odot}$ and $\zeta_{\kappa} = 0.175$).

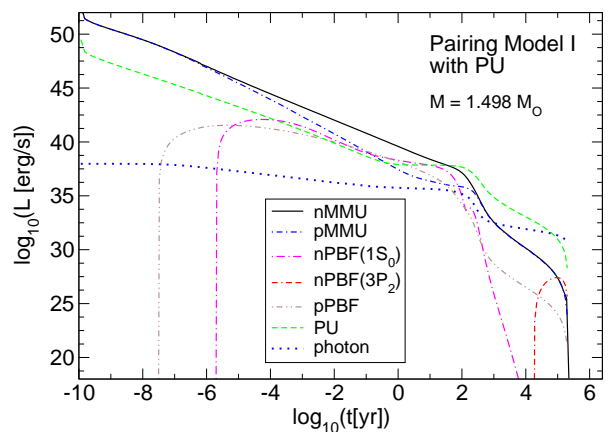


FIG. 6: (Color online) Individual contributions of the cooling processes, nMMU and pMMU, $1S_0$ pPBF and nPBF, $3P_2$ nPBF, PU, and surface photon emission, to the total stellar luminosity for the neutron star of mass $1.498 M_{\odot}$ shown in Fig. 5. Modeling with PU exploits curves 1a+2 for the pion excitations, and 3 determining the pion condensate amplitude in Fig. 1, pairing gaps from model I.

In Fig. 6 we show the individual contributions of the cooling processes in our scenario to the total neutron star luminosity for the neutron star with the mass $M = 1.498 M_{\odot}$, which best reproduces the new cooling data of Cas A in Fig. 5, for model I for pairing and PU model. We see that the nMMU and PU are the most efficient processes in this scenario, while $1S_0$ PBF processes are less important. Nevertheless they contribute at $t \lesssim 500$ yr. Although the MnB and MpB luminosities dominate over those of PBF in a broad time interval, they are not shown since they have rather similar shapes, as the nMMU and pMMU curves, but have smaller amplitudes. Note that PU processes control the neutron star cooling at later times ($300 \lesssim t/\text{yr} \lesssim 10^5$). For $t > 10^5$ yr the photon emission from the star surface is dominating.

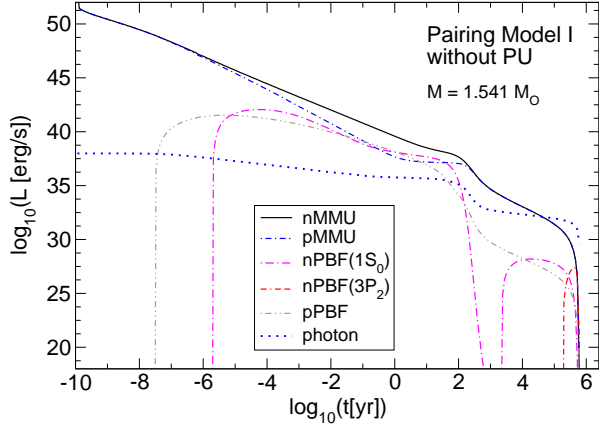


FIG. 7: (Color online) The same as in Fig. 6 but for the model “without PU”.

The $3P_2$ nPBF process is unimportant with values of the gap that we use.

In Fig. 7 we show the individual contributions of the cooling processes in our scenario to the total neutron star luminosity for the neutron star with mass $M = 1.541 M_\odot$, which best reproduces the new cooling data of Cas A in Fig. 5 for model I for pairing and without PU. We see that the nMMU are the most efficient processes in this scenario during the whole time evolution up to $t \lesssim 10^5$ yr. A little jump in the luminosity on the $1S_0$ nPBF at $10^3 \lesssim t/\text{yr} \lesssim 10^5$ is due to a still surviving inhomogeneity of the temperature profile at low densities, in the crust. This tiny effect does not influence the neutron star cooling evolution. It completely disappeared in the above considered PU model, where the mentioned temperature inhomogeneity is smoothed faster owing to more efficient heat transport.

IV. COOLING OF NEUTRON STARS WITH DIFFERENT MASSES

In Figs. 8 and 9 we demonstrate the general picture of the cooling of neutron stars with different masses for the model I for pairing. Fig. 8 shows cooling in the model, where PU processes are included, whereas Fig. 9, without PU. Although the overall picture is similar, in the model with PU presently available data are explained within an essentially narrower interval of neutron star masses ($1.39 < M/M_\odot < 1.5$) than in the model without PU ($1.39 < M/M_\odot < 1.9$). The cooling of stars with $M > M_{\text{DU}} = 1.881 M_\odot$ is controlled by the efficient DU process. The heaviest stars, which we now are able to describe with the HDD EoS, are cooled so fast that they are not seen in soft X -rays at least at present.

Fig. 10 shows the cooling of neutron stars with differ-

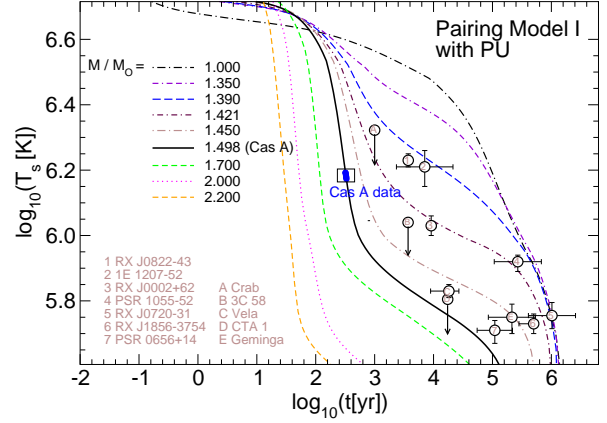


FIG. 8: (Color online) Cooling of neutron stars in the nuclear medium cooling scenario, with different masses within model I for pairing and with PU, cf. also Fig. 17 of [32] and Fig. 1 of [11]. Data from Refs. [9, 13]. New data for Cas A from [12].

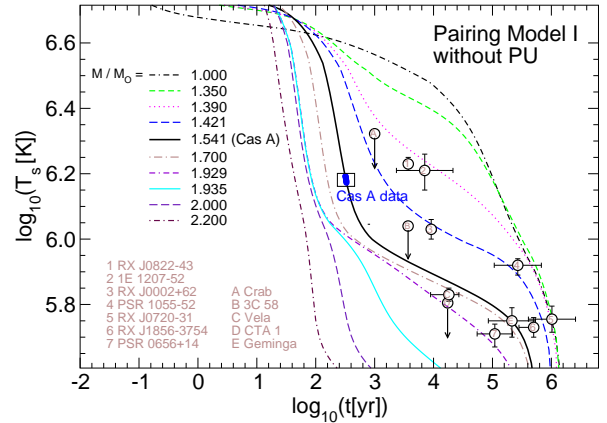


FIG. 9: (Color online) The same as in Fig. 8 but for the model without PU.

ent masses for the model II for pairing and for the model with PU. The 4% decline is not fitted without additional strong suppression of κ (in agreement with statement of [11] where we needed to suppress the thermal conductivity by factor $\zeta_\kappa \leq 0.015$ in order to describe a 4% decline with model II). However, the cooling curve corresponding to the star mass $M = 1.421 M_\odot$ matches the 2% decline (upper experimental border). Thus the scenario using model II still cannot be excluded at present. Subsequent measurements may allow to reduce the uncertainty in the decline, which will allow to distinguish between our scenarios using models I and II for pairing.

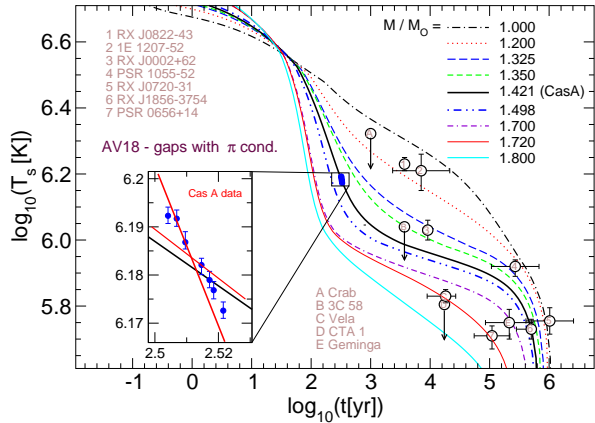


FIG. 10: (Color online) The same as in Fig. 8 but for the model II for pairing. Two extra lines in the inset frame show 2% and 5.5% declines.

V. SUMMARY AND CONCLUSION

We have shown in this paper that the nuclear medium cooling scenario allows one to nicely explain the observed rapid cooling of the neutron star in Cas A, as well as all other existing neutron star cooling data. As demonstrated already in [32] and then in [11], in our scenario the rapid cooling of very young objects like Cas A is mainly due to the efficient MMU processes, a very low (almost zero) value of the $3P_2$ neutron gap and a small thermal conductivity of neutron star matter. In the present work we do not use any artificial suppression parameter to demonstrate the effect of a small thermal conductivity caused by in-medium effects on Cas A cooling, but we *use the same values for the lepton thermal conductivity* as in Ref. [19]. The required smallness of thermal conductivity is provided by taking into account the collective effect of Landau damping.

We stress that, contrary to the minimal cooling models, within the nuclear medium cooling scenario we are trying to consistently include the most important collective effects in all relevant processes – the pion softening effect in the NN interaction amplitude [17], collective effects in the pair-breaking-formation processes [42], collective effects in the pairing gaps, the screening effect in the lepton contribution to the thermal conductivity [21] and a decrease of the nucleon contribution owing to the mentioned pion softening, etc. And we did not introduce any significant changes in our scenario developed in 2004 in [32], except for including the suppression of the thermal conductivity, now performed as in [19]. Thus in difference with other scenarios, explanation of the Cas A data straightly follows the predictions of our previous work [32].

The pion softening effect manifesting itself in an in-

crease of the NN interaction amplitude with growing density [16, 17] causes a decrease of the nucleon contribution to the thermal conductivity and at the same time leads to a strong enhancement of the emissivities of two-nucleon neutrino processes [17, 27]. With due account of exact vector current conservation the pair-breaking-formation processes on the vector current prove to be dramatically suppressed [41] and operate instead on the axial current [42], for which the suppression effect is less pronounced. Following calculations of [18] which take into account polarization effects, the $3P_2$ gap is dramatically suppressed. The screening effect taken into account in the calculation of the lepton thermal conductivity [19] leads to its strong suppression compared to the earlier result of Ref. [20]. We included only the most efficient in-medium processes. However, the results are sensitive to details of the description of strong interactions in dense matter. Thus demonstrating nice agreement with the data we only argue in favor of a general picture but not guarantee quantitative values of all involved quantities. There are still many other in-medium reaction channels which we did not include in the code. For example, in superfluid matter spin excitonic and diffusive modes [57] and massive photon decay [58] may contribute, while in pasta phases DU-like processes on structures [53] may operate, the nucleon Fermi sea may be rearranged in the vicinity of the pion condensation point [59]. We did not consider possibilities of other phase transitions except pion condensation. Unfortunately, quantitative estimates of these processes depend on the values of some not well known parameters. Therefore, we postpone their inclusion in the cooling code in order not to multiply uncertainties.

Thus our explanation of the Cas A cooling constitutes an alternative to that of [8, 10, 12], which is based on a strong nPBF process due to $3P_2$ superfluidity in neutron star interiors and suppressed emissivities of pPBF and MU two-nucleon processes operating on the charged current by a suggestion to use a large proton gap. The conclusion that from Cas A observations one is able to recover the value of the $3P_2$ nn -pairing gap seems to us misleading, due to the existence of other (not exotic!) possibilities to explain Cas A, as well as all other available cooling data. We support, however, the conclusion of these authors about the sensitivity of the result to the chosen value of the proton gap. In our scenario this occurs due to the sensitivity of the MMU emissivity to the value and the density dependence of the proton gap spreading up to $n \lesssim 3 \dots 4n_0$ in the neutron star core, where the MMU process is most efficient. We got the best (4% decline) fit of Cas A data with a larger proton gap (model I). Nice overall agreement with available cooling data is achieved with a tiny $3P_2$ nn pairing gap and it would be destroyed, if we used values of the $3P_2$ pairing gap similar to those used in [8, 10, 12].

Alternative explanations include the suggestion [60] that Cas A is a rapidly rotating star and during its spin-down the efficient DU process is switched on when the

redistribution of matter leads to an increase of the central density beyond the DU threshold. Ref. [61] suggests that Cas A is a hybrid star. However, note that except our scenario other works aiming at a description of Cas A do not demonstrate their capability to obtain in the framework of the same assumptions an overall agreement with other available neutron star cooling data.

Further tests may be considered, such as a comparison of log N-log S distributions from population synthesis with the observed one for isolated neutron stars [62]. Also a continuation of the measurements of Cas A and new measurements of neutron star temperatures are welcome to discriminate between alternative cooling scenarios.

In this paper we also incorporated an excluded volume effect in the HHJ($\delta = 0.2$) EoS thus extending our previous works in order to describe the cooling of stars with masses $\gtrsim 2 M_{\odot}$. We demonstrated that a difference of the here constructed HDD EoS with the HHJ($\delta = 0.2$) EoS appears only for densities $> 4n_0$. Thereby only the

cooling curves starting from $M \sim 1.6 M_{\odot}$ are affected by this change of the EoS. The HDD EoS might be helpful to study hybrid stars, owing to its additional stiffening at densities exceeding $4n_0$, when a phase transition to quark matter is expected [63]. We hope to return to this analysis in a forthcoming publication.

Acknowledgments

We thank E. E. Kolomeitsev and F. Weber for discussions. This work was supported by Narodowe Centrum Nauki under contract No. DEC-2011/02/A/ST2/00306 and by CompStar, a research networking programme of the European Science Foundation. D.B. has been supported by RFBR under grant No. 11-02-01538-a and H.G. acknowledges support by the Volkswagen Foundation under grant No. 85 182.

-
- [1] H. Tananbaum, IAU Circ., **7246**, 1 (1999); J. P. Hughes, C. E. Rakowski, D. N. Burrows, and P. O. Slane, *Astrophys. J. Lett.* **528**, L109 (2000).
 - [2] W. B. Ashworth, Jr., *J. Hist. Astron.* **11**, 1 (1980).
 - [3] R. A. Fesen, M. C. Hammell, J. Morse, R. A. Chevalier, K. J. Borkowski, M. A. Dopita, C. L. Gerardy, S. S. Lawrence, J. C. Raymond, and S. van den Bergh, *Astrophys. J.* **645**, 283 (2006).
 - [4] W. C. G. Ho and C. O. Heinke, *Nature* **462**, 71 (2009).
 - [5] C. O. Heinke and W. C. G. Ho, *Astrophys. J. Lett.* **719**, L167 (2010).
 - [6] D. G. Yakovlev, A. D. Kaminker, O. Y. Gnedin and P. Haensel, *Phys. Rept.* **354**, 1 (2001).
 - [7] D. Page, U. Geppert and F. Weber, *Nucl. Phys. A* **777**, 497 (2006).
 - [8] D. Page, M. Prakash, J. M. Lattimer and A. W. Steiner, *Phys. Rev. Lett.* **106**, 081101 (2011).
 - [9] D. G. Yakovlev, W. C. G. Ho, P. S. Shternin, C. O. Heinke and A. Y. Potekhin, *Mon. Not. Roy. Astron. Soc.* **411**, 1977 (2011).
 - [10] P. S. Shternin, D. G. Yakovlev, C. O. Heinke, W. C. G. Ho and D. J. Patnaude, *Mon. Not. Roy. Astron. Soc.* **412**, L108 (2011).
 - [11] D. Blaschke, H. Grigorian, D. N. Voskresensky and F. Weber, *Phys. Rev. C* **85**, 022802 (2012).
 - [12] K. G. Elshamouty, C. O. Heinke, G. R. Sivakoff, W. C. G. Ho, P. S. Shternin, D. G. Yakovlev, D. J. Patnaude and L. David, *Astrophys. J.* **777**, 22 (2013).
 - [13] D. Page, J. M. Lattimer, M. Prakash and A. W. Steiner, *Astrophys. J. Supp.* **155**, 623 (2004); *Astrophys. J.* **707**, 1131 (2009).
 - [14] B. L. Friman and O. V. Maxwell, *Astrophys. J.* **232**, 541 (1979).
 - [15] D. Page, arXiv:1206.5011 [astro-ph.HE].
 - [16] A. B. Migdal, *Rev. Mod. Phys.* **50**, 107 (1978).
 - [17] A. B. Migdal, E. E. Saperstein, M. A. Troitsky and D. N. Voskresensky, *Phys. Rept.* **192**, 179 (1990).
 - [18] A. Schwenk and B. Friman, *Phys. Rev. Lett.* **92**, 082501 (2004).
 - [19] P. S. Shternin and D. G. Yakovlev, *Phys. Rev. D* **75**, 103004 (2007).
 - [20] D. A. Baiko, P. Haensel and D. G. Yakovlev, *Astron. Astrophys.* **374**, 151 (2001); O. Y. Gnedin and D. G. Yakovlev, *Nucl. Phys.* **A582**, 697 (1995).
 - [21] H. Heiselberg and C. J. Pethick, *Phys. Rev. D* **48**, 2916 (1993).
 - [22] P. Jaikumar, C. Gale and D. Page, *Phys. Rev. D* **72**, 123004 (2005).
 - [23] H. Heiselberg and M. Hjorth-Jensen, *Astrophys. J.* **525**, L45 (1999).
 - [24] A. Akmal, V. R. Pandharipande and D. G. Ravenhall, *Phys. Rev. C* **58**, 1804 (1998).
 - [25] P. Demorest, T. Pennucci, S. Ransom, M. Roberts and J. Hessels, *Nature* **467**, 1081 (2010).
 - [26] J. Antoniadis, P. C. C. Freire, N. Wex, T. M. Tauris, R. S. Lynch, M. H. van Kerkwijk, M. Kramer and C. Bassa, *Science* **340**, 6131 (2013).
 - [27] D. N. Voskresensky and A. V. Senatorov, *Sov. Phys. JETP* **63**, 885 (1986); *JETP Lett.* **40**, 1212 (1984).
 - [28] D. N. Voskresensky and A. V. Senatorov, *Sov. J. Nucl. Phys.* **45**, 411 (1987); A. V. Senatorov and D. N. Voskresensky, *Phys. Lett. B* **184**, 119 (1987).
 - [29] D. N. Voskresensky, *Lect. Notes Phys.* **578**, 467 (2001).
 - [30] E. E. Kolomeitsev and D. N. Voskresensky, *Phys. Atom. Nucl.* **74**, 1316 (2011).
 - [31] C. Schaab *et al.*, *Astron. Astrophys.* **321**, 591 (1997).
 - [32] D. Blaschke, H. Grigorian and D. N. Voskresensky, *Astron. Astrophys.* **424**, 979 (2004).
 - [33] H. Grigorian and D. N. Voskresensky, *Astron. Astrophys.* **444**, 913 (2005).
 - [34] H. Grigorian, *Phys. Rev. C* **74**, 025801 (2006).
 - [35] D. Blaschke, G. Röpke, H. Schulz, A. D. Sedrakian and D. N. Voskresensky, *Mon. Not. Roy. Astron. Soc.* **273**, 596 (1995).
 - [36] C. Hanhart, D. R. Phillips and S. Reddy, *Phys. Lett. B* **499**, 9 (2001).
 - [37] T. L. Ainsworth, J. Wambach and D. Pines, *Phys. Lett. B* **222**, 173 (1989).

- [38] D. G. Yakovlev, O. Y. Gnedin, A. D. Kaminker, K. P. Levenfish and A. Y. Potekhin, *Adv. Space Res.* **33**, 523 (2004).
- [39] T. Takatsuka and R. Tamagaki, *Prog. Theor. Phys.* **112**, 37 (2004).
- [40] E. Flowers, M. Ruderman and P. Sutherland, *Astrophys. J.* **205**, 541 (1976).
- [41] L. B. Leinson and A. Perez, *Phys. Lett. B* **638**, 114 (2006).
- [42] E. E. Kolomeitsev and D. N. Voskresensky, *Phys. Rev. C* **77**, 065808 (2008); *Phys. Rev. C* **81**, 065801 (2010).
- [43] C. Shen, U. Lombardo and P. Schuck, *Phys. Rev. C* **67**, 061302 (2003).
- [44] W. Zuo, Z. H. Li, G. C. Lu, J. Q. Li, W. Scheid, U. Lombardo, H. J. Schulze and C. W. Shen, *Phys. Lett. B* **595**, 44 (2004).
- [45] X. -R. Zhou, H. -J. Schulze, E. -G. Zhao, F. Pan and J. P. Draayer, *Phys. Rev. C* **70**, 048802 (2004).
- [46] M. Baldo and H. -J. Schulze, *Phys. Rev. C* **75**, 025802 (2007).
- [47] W. Zuo and G. C. Lu, *Phys. Rev. C* **75**, 045806 (2007).
- [48] W. Zuo, C. X. Cui, U. Lombardo and H. -J. Schulze, *Phys. Rev. C* **78**, 015805 (2008).
- [49] J. M. Dong, U. Lombardo and W. Zuo, *Phys. Rev. C* **87**, 062801 (2013).
- [50] V. A. Khodel, J. W. Clark, M. Takano and M. V. Zverev, *Phys. Rev. Lett.* **93**, 151101 (2004).
- [51] T. Maruyama *et al.*, *Phys. Rev. C* **72**, 015802 (2005).
- [52] W. G. Newton, K. Murphy, J. Hooker and B. -A. Li, arXiv:1308.2137 [astro-ph.SR].
- [53] L. B. Leinson, *JETP Lett.* **57**, 265 (1993); M. E. Gusakov, D. G. Yakovlev, P. Haensel and O. Y. Gnedin, *Astron. Astrophys.* **421**, 1143 (2004).
- [54] D. G. Yakovlev, K. P. Levenfish, A. Y. Potekhin, O. Y. Gnedin and G. Chabrier, *Astron. Astrophys.* **417**, 169 (2004).
- [55] P. Danielewicz, R. Lacey and W. G. Lynch, *Science* **298**, 1592 (2002).
- [56] T. Klähn, *et al.*, *Phys. Rev. C* **74**, 035802 (2006).
- [57] E. E. Kolomeitsev and D. N. Voskresensky, *Phys. Rev. C* **84**, 068801 (2011).
- [58] D. N. Voskresensky, E. E. Kolomeitsev and B. Kämpfer, *J. Exp. Theor. Phys.* **87**, 211 (1998).
- [59] D. N. Voskresensky, V. A. Khodel, M. V. Zverev and J. W. Clark, *Astrophys. J.* **533**, 127 (2000).
- [60] R. Negreiros, S. Schramm and F. Weber, *Phys. Lett. B* **718**, 1176 (2013).
- [61] A. Sedrakian, *Astron. Astrophys.* **555**, L 10 (2013).
- [62] S. Popov, H. Grigorian, R. Turolla and D. Blaschke, *Astron. Astrophys.* **448**, 327 (2006).
- [63] T. Klähn, D. B. Blaschke and R. Lastowiecki, *Phys. Rev. D* **88**, 085001 (2013).